



Tetrapropylammonium Hydroxide as a Zinc Dendrite Growth Suppressor for Rechargeable Aqueous Battery

Indira Kurmanbayeva^{1,2*}, Lunara Rakhymbay¹, Kuralay Korzhynbayeva^{1,2}, Akylbek Adi¹, Dauren Batyrbekuly¹, Almagul Mentbayeva^{2,3} and Zhumabay Bakenov^{1,2,3}

¹National Laboratory Astana, Nur-Sultan, Kazakhstan, ²Institute of Batteries LLC, Nur-Sultan, Kazakhstan, ³Nazarbayev University, Nur-Sultan, Kazakhstan

OPEN ACCESS

Edited by:

Soorathep Kheawhom,
Chulalongkorn University, Thailand

Reviewed by:

Cheng Zhong,
Tianjin University, China
Ning Zhang,
Hebei University, China

*Correspondence:

Indira Kurmanbayeva
indira.kurmanbayeva@nu.edu.kz

Specialty section:

This article was submitted to
Electrochemical Energy Conversion
and Storage,
a section of the journal
Frontiers in Energy Research

Received: 26 August 2020

Accepted: 27 October 2020

Published: 24 November 2020

Citation:

Kurmanbayeva I, Rakhymbay L,
Korzhynbayeva K, Adi A, Batyrbekuly
D, Mentbayeva A and Bakenov Z
(2020) Tetrapropylammonium
Hydroxide as a Zinc Dendrite Growth
Suppressor for Rechargeable
Aqueous Battery.
Front. Energy Res. 8:599009.
doi: 10.3389/fenrg.2020.599009

Zinc metal is widely used as an anode in various aqueous systems. However, zinc anode suffers from the dendrite formation on the surface upon cycling leading to a poor cyclability of a cell and its termination due to short circuit. In this work, the effect of tetrapropylammonium hydroxide (TPAH) was studied as an electrolyte additive for aqueous Zn//ZnCl₂ + LiCl/LiFePO₄ battery. TPAH additive prolongs the battery cycle life depending on its concentration (0.01–0.1 M). The better capacity retention over 350 cycles was observed for a symmetrical Zn//ZnCl₂ + LiCl/Zn cell with 0.05 M TPAH whereas without additives the cell worked for only 110 cycles. The mechanism of TPAH influence on capacity retention is proposed based on the results of SEM and XRD analysis of the Zn anode and FTIR and NMR studies of the electrolyte. The XRD patterns of the negative electrode of the cell with TPAH indicates that zinc was preferentially deposited in a highly oriented (002) direction, which is more resistant against dendrite formation. These differences in deposited structure of Zn dendrites were confirmed by SEM images as well. FTIR and NMR spectra showed that TPAH decomposes to propylamine (R_nN⁺H) and propene during cycling. TPAH also has an effect on the size and uniform distribution of Zn growth sides.

Keywords: tetrapropylammonium hydroxide, zinc anode, zinc dendrites suppression, aqueous electrolyte, lithium-ion battery

INTRODUCTION

Zinc metal is considered as a promising anode material for rechargeable battery due to its high theoretical capacity (820 mAh g⁻¹), abundance, safety, scalability, low cost, and environmental friendliness (Zhang et al., 2017; Fang et al., 2018; Wang et al., 2018a; Li et al., 2019a; Zhang et al., 2020). Zinc based anode materials are used in such systems as zinc-manganese (Beck and Rüetschi, 2000; Zhu et al., 2018), zinc-air (Wang et al., 2018b), nickel-zinc (Moser et al., 2013; Parker et al., 2017), zinc-vanadium based battery (Hu et al., 2017; Batyrbekuly et al., 2020), and so forth. According to the Pourbaix diagram (Konarov et al., 2018; Li et al., 2019a; Zeng et al., 2019; Shin et al., 2020) zinc is thermodynamically unstable in the aqueous environment. It dissolves into Zn²⁺ ions under acidic conditions (pH < 4), it is more stable at neutral pH, and its solubility increases in alkaline media. Commercial, mainly used as primary batteries, aqueous zinc batteries (Zn-air, Zn-MnO₂, etc.) have alkaline media (Yufit et al., 2019; Zhang et al., 2020), where Zn(OH)₄⁻² complexes formed due to the abundance of OH⁻ ions. These zincate ions precipitate in the form of ZnO, resulting in dendrite growth or passivation of the anode. Mildly acidic aqueous (or neutral)

electrolyte for lithium-ion batteries is being investigated relatively recently (Xu et al., 2012; Yan et al., 2012; Zhang et al., 2017; Li et al., 2019a). Xu et al. (2012) show that the replacement of alkaline electrolyte to mild acidic in the Zn-MnO₂ battery changed the chemistry. In mild acidic media, Zn²⁺ ions are reduced and deposited in Zn metallic form, leaving place for side reaction (corrosion). However, nonuniform growth of dendrites and corrosion during cycling still prevents the widespread use of the zinc anode. Numerous works have been investigated to suppress the Zn dendrite formation, such as the modification of the zinc electrode surface (Wang et al., 2019; Zhou et al., 2019) or adding an organic and inorganic additive into electrolyte (Lan et al., 2007; Bani Hashemi et al., 2017).

Hoang et al. designed a hydrogel electrolyte (based on 1 M Li₂SO₄ and 2 M ZnSO₄) with fumed silica and PbSO₄ for Zn/LiMn₂O₄ cell. This gel electrolyte acts as a corrosion inhibitor and dendrite suppressor (Hoang et al., 2017). Organic molecules are commonly used additives to the electrolyte to suppress the Zn dendrite formation. According to the literature, they coordinate or complex with zinc ions (Xu et al., 2015; Wang et al., 2018c). Mitha et al. improved the electrochemical performances of Zn/LiMn₂O₄ rechargeable aqueous battery by adding of polyethylene glycol (PEG200) in Li₂SO₄ and ZnSO₄ electrolyte by approximately 32% in comparison with control sample (Mitha et al., 2018; Mitha et al., 2019). Kan et al. (1998) compared the effect of adding PbCl₂, sodium lauryl sulfate, and Triton X-100 to the electrolyte (2 M NH₄Cl and 2.5 M ZnCl₂) for Zn/polyaniline secondary battery, where Triton X-100 showed the most promising results. Lan et al. (2007) described the study of several tetraalkylammonium hydroxides as Zn dendrite's inhibition additives to alkaline 0.45 M ZnO + 6.6 M KOH electrolyte. Authors claim that inhibition of dendrites is positively correlated with the size of alkyl group of alkyl ammonium hydroxides. The authors claim that inhibition of dendrites is positively correlated with the size of alkyl group of alkylammonium hydroxides. The polarity of tetraalkylammonium hydroxides should be not too strong or too weak to uniformly cover the Zn electrode surface. 0.01 M TPAH was found as the best and ecologically friendly Zn dendrite inhibitor (Lan et al., 2007). The mechanism of zinc dendrites in alkaline electrolyte underlying the suppression of dendrite growth is related to the ability of additives to be absorbed on the surface of the electrode (Lan et al., 2007; Garcia et al., 2017; Lu et al., 2018; Li et al., 2019b). Ammonium based additives in electrolytes slowed down diffusional mass transport, were adsorbed on the specific sites of the electrode, and blocked the rapid growth of Zn dendrites via steric hindrance. That is why it was interesting to investigate the tetrapropylammonium hydroxide (TPAH) as Zn dendrite inhibitor in lithium-ion Zn/LiFePO₄ battery with mild acid aqueous electrolyte (pH = 4), containing 4 M ZnCl₂ and 3 M LiCl. The mechanism of TPAH interaction with electrolyte and Zn anode during cycling is proposed based on the results of SEM and XRD analysis of the Zn anode and FTIR and NMR studies of the electrolyte.

MATERIAL AND METHODS

Materials

LiFePO₄ (MTI, Corp., China), Ketjen black (Ketjen Black International, Co., Japan), and polyvinylidene fluoride (PVDF, Kynar, HSV900), 1-methyl-2-pyrrolidinone (NMP, Sigma-Aldrich), carbon fiber paper (Alfa Aesar, Co.), Cu foil with 30 μm thickness (MTI Corporation, United States), Zn foil with 100 μm thickness (Goodfellow, United States), LiCl (Sigma-Aldrich), ZnCl₂ (Sigma-Aldrich), TPAH (Sigma-Aldrich), and AGM (Adsorptive Glass Mat, NSG Corporation) were used.

Materials Preparation and Battery Cell Assembling

The electrodes and reference electrolyte were prepared as described in our previous work (Yesibolati et al., 2015). Briefly, to prepare a positive electrode an appropriate amount of LiFePO₄, Ketjen black, and PVDF, dissolved in NMP (90:4:6 wt %), were mixed to get homogeneous slurry. The slurry was then casted on carbon fiber paper and vacuum-dried at 70°C for 2 h in a vacuum oven and punched disks with 6 mm diameter. As a reference and counter electrode Zn foil discs with 8 mm diameter were used. The reference electrolyte was prepared by dissolving 3 M LiCl and 4 M ZnCl₂ in deionized water. TPAH was then introduced into the electrolyte at different concentrations. The pH of the electrolyte was adjusted to 4 by LiOH and HCl.

To study Zn dendrite suppression ability and mechanism of TPAH, three types of cells were assembled in this work.

Swagelok-type Zn//ZnCl₂ + LiCl//LiFePO₄ half cells were assembled in accordance with our previous report (Yesibolati et al., 2015). The assembled cells were galvanostatically cycled on a NEWARE battery tester (Neware Co, Ltd., China) in the potential window of 1.0–1.4 V at a current density of 0.1 C (1 C = 170 mAh g⁻¹). Cyclic voltammetry (CV) was performed with a VMP3 potentiostat/galvanostat (BioLogic Science Instrument, Co., France) in the potential window of 1.0–1.4 V at a scan rate of 0.1 mV s⁻¹.

Swagelok-type Zn//ZnCl₂ + LiCl//Zn symmetric cells were assembled in a similar way to the above half cells. The LiFePO₄ positive electrode was replaced by the Zn disk with 8 mm diameter. Every charge/discharge cycling was carried out in 30 min at a current density of 1 mA cm⁻².

Beaker cell-type Zn//ZnCl₂ + LiCl//Cu cell was assembled to further study the zinc dendrite suppression mechanism by organic additives (TPAH). A zinc foil was used as a reference and counter electrode, and a copper foil served as a current collector for plating/stripping of a known amount of zinc. Both electrodes were 15 mm in diameter and separated by AGM glass separator. The electrodes were half-immersed into an aqueous electrolyte of 3/4 M lithium/zinc chlorides with and without TPAH. The assembled beaker cells were galvanostatically cycled using a BioLogic battery tester. In the first discharge, 1 mAh (or approximately 1.2 mg) Zn was deposited onto Cu foil, and then it was stripped during the charging up to 0.8 V (Higashi et al., 2016).

All electrochemical characterizations were performed at a room temperature.

Characterization

The morphology of the Zn electrodes was observed by Field emission scanning electron microscopy (FE-SEM, JEOL, JSM-7500F). X-Ray diffractometer (Rigaku SmartLab) was applied to identify phases on the surface of anode after cycling. The cycled Zn electrodes were washed by distilled water to remove residual electrolyte. The electrolyte solutions were analyzed by Fourier Transform Infrared Spectroscopy (Nicolet iS10 FT-IR) and FT NMR spectrometer (JEOL, ECA-500).

RESULTS AND DISCUSSION

To check a possible impact of TPAH on the electrochemical performance of the aqueous Zn//ZnCl₂ + LiCl//LiFePO₄ battery system, the cyclic voltammetry was performed for the cells with and without TPAH electrolyte additives. **Figure 1** shows CV profiles of the Zn//ZnCl₂ + LiCl//LiFePO₄ cells without and with 0.1 M TPAH in the potential window of 1.0–1.4 V at 0.1 mV s⁻¹ for initial first, third, and fifth cycles.

Both cells had a single redox pair corresponding to lithiation/delithiation of LiFePO₄ at 1.14/1.28 V, respectively (Yesibolati et al., 2015). The absence of additional peaks in the CV curves of the cell with the electrolyte additive (**Figure 1B**) indicated that TPAH additive has no negative effect on the electrochemical reactions in aqueous Zn//ZnCl₂ + LiCl//LiFePO₄ battery system.

The Zn plating/stripping behavior was studied using the Zn//ZnCl₂ + LiCl//Zn symmetric cell without additive and with TPAH at different concentrations (0.01, 0.02, 0.05, and 0.1 M). **Figure 2** a shows the voltage versus time profiles of the symmetric cells without and with 0.05 M TPAH electrolyte additive at a current density of 1 mA cm⁻². The cell without TPAH electrolyte additive had lower polarization (less than 0.1 V) in the initial 40 h. However, the cell polarization increased to 0.45 V at a later time and the cell short-circuited by 60 h. On the other hand, the cell with TPAH electrolyte additive had a larger polarization (0.3 V) from the initial hours due to an increased resistance of the Zn electrode with adsorbed TPAH molecules (Garcia et al., 2017; Lu et al., 2018). The use of 0.05 M TPAH additive prolonged the cyclability of symmetric cell up to 352 cycles (or 180 h). The cell with lower concentration of TPAH (0.01 M, 0.02 M) overperformed the cell without the additive (**Supplementary Figure S1**). However, a further increasing of the additive concentration (0.1 M) had no significant improvement on the symmetric cell cycle life (**Supplementary Figure S1**).

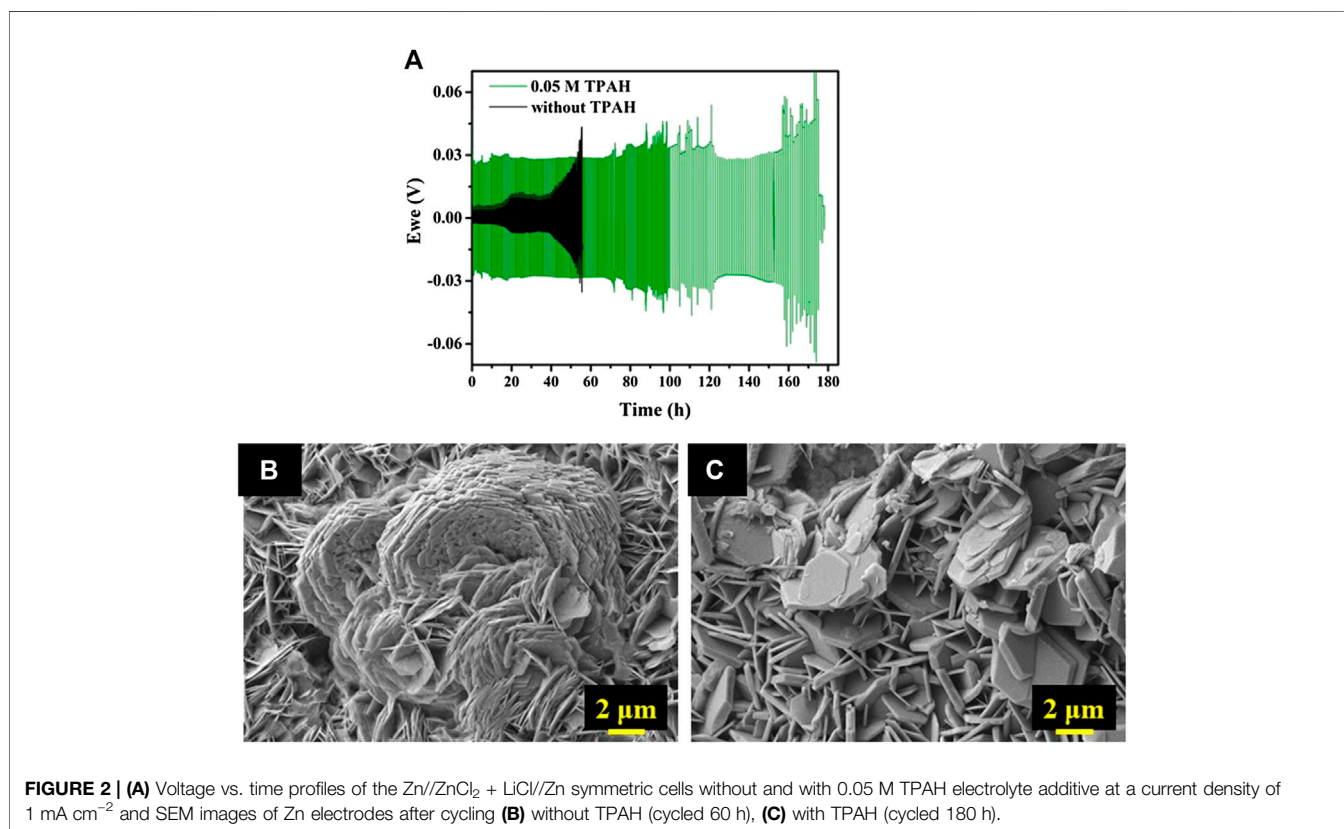
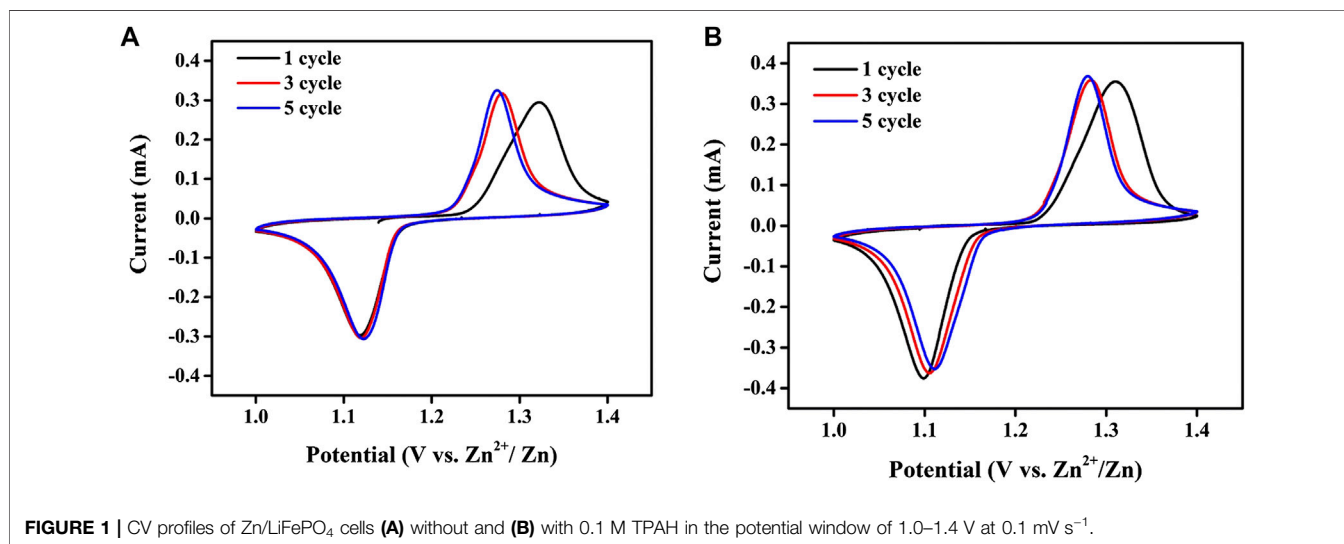
Figures 2B,C present the SEM images of the Zn electrodes in symmetric cells without and with TPAH additive, respectively. Randomly oriented Zn hexagonal disks with average size 1–3 μm can be seen on the surface of both electrodes. Zn dendrite has grown into flower-like agglomerate with a size of approximately 18–20 μm in width on the additive-free symmetric cell, which cycled 60 h (**Figure 2B**). Only hexagonal Zn disks (mostly horizontally oriented) are seen from the image of anode with 0.05 M TPAH addition (**Figure 2C**). The TPAH additive prevents

such big Zn dendrite growth even though the cell cycled for about 180 h. Zn disks in **Figure 2C** just have become thicker.

In order to understand the positive effect of TPAH on Zn dendrite suppression, the large-scaled beaker cell-type Zn//ZnCl₂ + LiCl//Cu battery was designed and assembled (**Supplementary Figure S2**). Increasing of TPAH concentration two times (0.02 M) does not give twice improvement of the cell cyclability, the same situation for 0.05 M additive concentration. Increased concentrations will not be economically effective as with 0.01 M TPAH. Due to this, the 0.01 M concentration was chosen for further investigation. Using a copper foil as a current collector instead of a zinc foil allows for quantifying an amount of Zn deposited onto Cu foil and then calculating the Coulombic efficiency. In the first discharge, 1.2 mg Zn was deposited onto Cu foil, and then it was charged until 0.8 V during which the deposited zinc stripped from Cu foil (Higashi et al., 2016). **Figures 3A,B** show charge/discharge curves of the cells without and with 0.01 M TPAH electrolyte additive, respectively, at a current density of 20 mA cm⁻². The cell without TPAH additive demonstrated a stable zinc deposition/stripping performance up to 50 cycles with an overpotential of ~120 mV (**Figure 3A**). However, a sharp decrease of overpotential from ~120 to ~60 mV occurred after 50 cycles associated with a short circuit of the cell, whereas the presence of TPAH additive in the electrolyte improved cycle stability of the cell over 70 cycles due to its zinc dendrite suppression effect (**Figure 3B**) (**Supplementary Figure S5**).

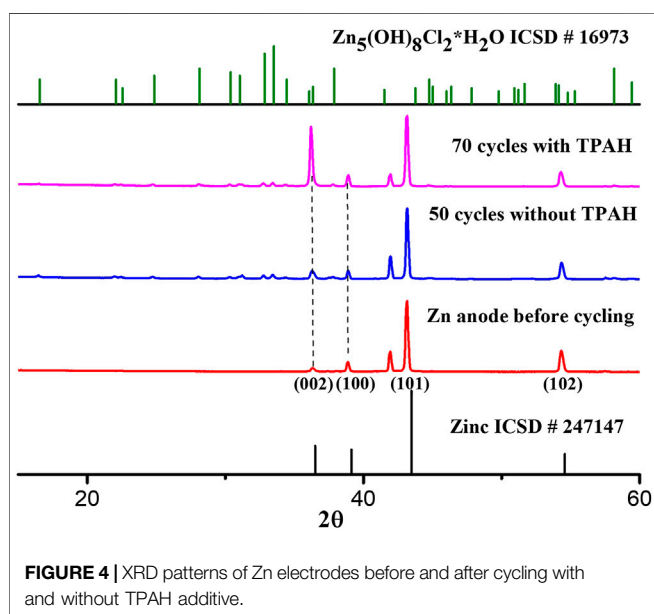
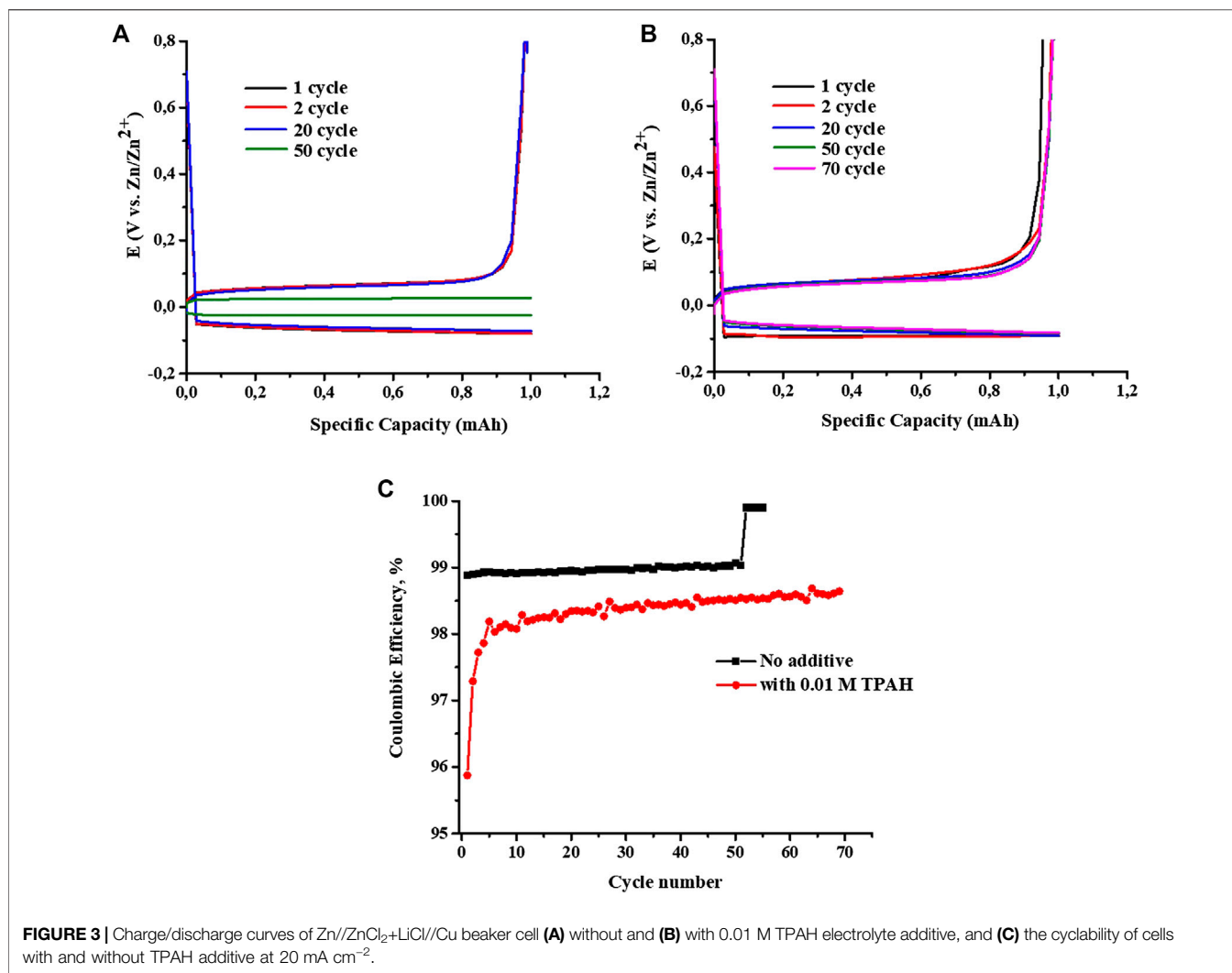
Figure 3C shows Coulombic efficiency versus cycle number profiles of the beaker cells without and with TPAH additive. The beaker cell without TPAH additive had a constant Coulombic efficiency of 99% over 50 cycles, while the Coulombic efficiency of the cell with TPAH additive fluctuated in the initial cycles and then stabilized to 98.5% in the subsequent cycles. However, the cell without TPAH additive short-circuited after 50 cycles with an abrupt increase of the Coulombic efficiency, whereas the cell with TPAH additive demonstrated a stable cycle performance. The improved cycle stability of the cell further confirms a significant effect of TPAH additive on zinc dendrite suppression. To study the mechanism of TPAH additive for the dendrite suppression, the electrodes and electrolyte were analyzed by many characterization techniques before and after cycling.

Dendrite deposition behavior of both Zn electrodes after cycling was investigated by XRD. **Figure 4** demonstrates XRD patterns of the Zn electrodes before and after cycling with and without TPAH additive. The pattern obtained on both electrodes after cycling has no significant difference from pure Zn reference, suggesting reversible behavior of Zn deposition/dissolution. Significant lattice planes (002), (100), (101), and (102) are identical with a literature (Gomes and da Silva Pereira, 2006; Nayana and Venkatesha, 2011; Nayana and Venkatesha, 2015) and demonstrate the different directions of crystal growth. The highest intensity peak at 42° indicated Zn growth in mostly directed (101) orientation, which causes the formation of tips (Nayana and Venkatesha, 2015). However, the intensity of (002) peak of Zn anode with TPAH addition increases, indicating that zinc was preferentially deposited in a basal (parallel) oriented direction



to anode surface, which is more resistant against dendrite formation (Sun et al., 2018). Similar behavior of nitrogen-containing amine group of CTAB (cetyltrimethylammonium bromide) was investigated in zinc electrodeposition by Nayana (Nayana and Venkatesha, 2011). This may explain the good battery performance of battery with TPAH addition due to the more 002 oriented deposited zinc.

An additional phase in the XRD patterns was observed and identified as simonkolleite (Zn₅(OH)₈Cl₂ · H₂O) in both anodes after cycling (**Supplementary Figure S4**). This also was confirmed by EDS mapping of cycled Zn anodes with/without TPAH, which shows the presence of Zn, O, and Cl (**Supplementary Figure S3**). It can be noted that simonkolleite, which acts as a corrosion stabilizer, forms in



case of high Cl content and low pH value (Yoo et al., 2013; Cousy et al., 2017; Li et al., 2019c).

The comparison of Zn electrode surface morphology cycled in beaker cells with and without TPAH addition was done by SEM. It is clearly seen from SEM images that the Zn electrode surfaces of both beaker cells have dendrites, but the character of deposition is different (**Figures 5A,B**). It can be seen from images with small magnification that Zn anode of cell without TPAH has uneven growth of dendrites; they are almost located on the right side (**Figure 5A**). Due to the growth upon cycling and penetration of dendrites into AGM separator, it was not possible to detach. The fibers of the separator are seen in the picture, whereas the left corner of the image is clean from dendrites. The Zn dendrites are more uniformly distributed on the anode surface in case of battery with TPAH addition. The size of dendrites is smaller (**Figure 5B**) and, as a result, this cell worked longer for 20 cycles at 20°C in comparison with battery without TPAH. The larger magnification shows that dendrites of the anode without TPAH have a compact structure with closely packed Zn disks (**Figure 5C**), whereas TPAH addition makes these dendrites

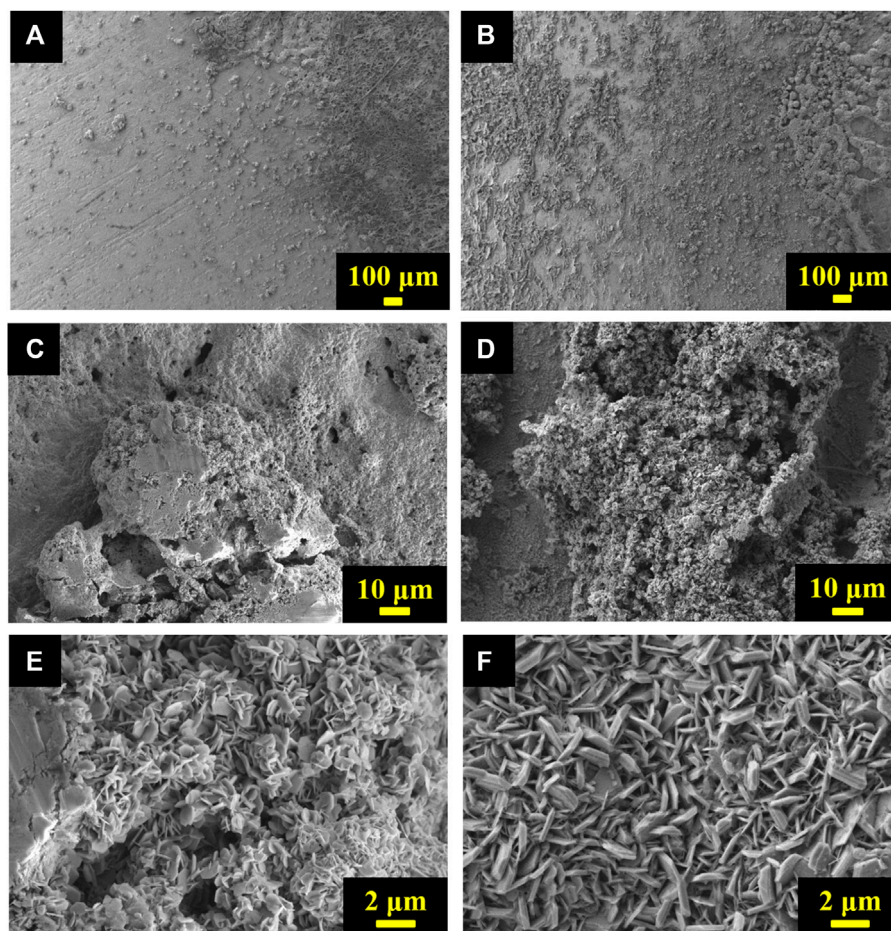


FIGURE 5 | SEM images of cycled Zn anodes (**A,C,E**) without TPAH and (**B,D,F**) with TPAH additive at different magnifications.

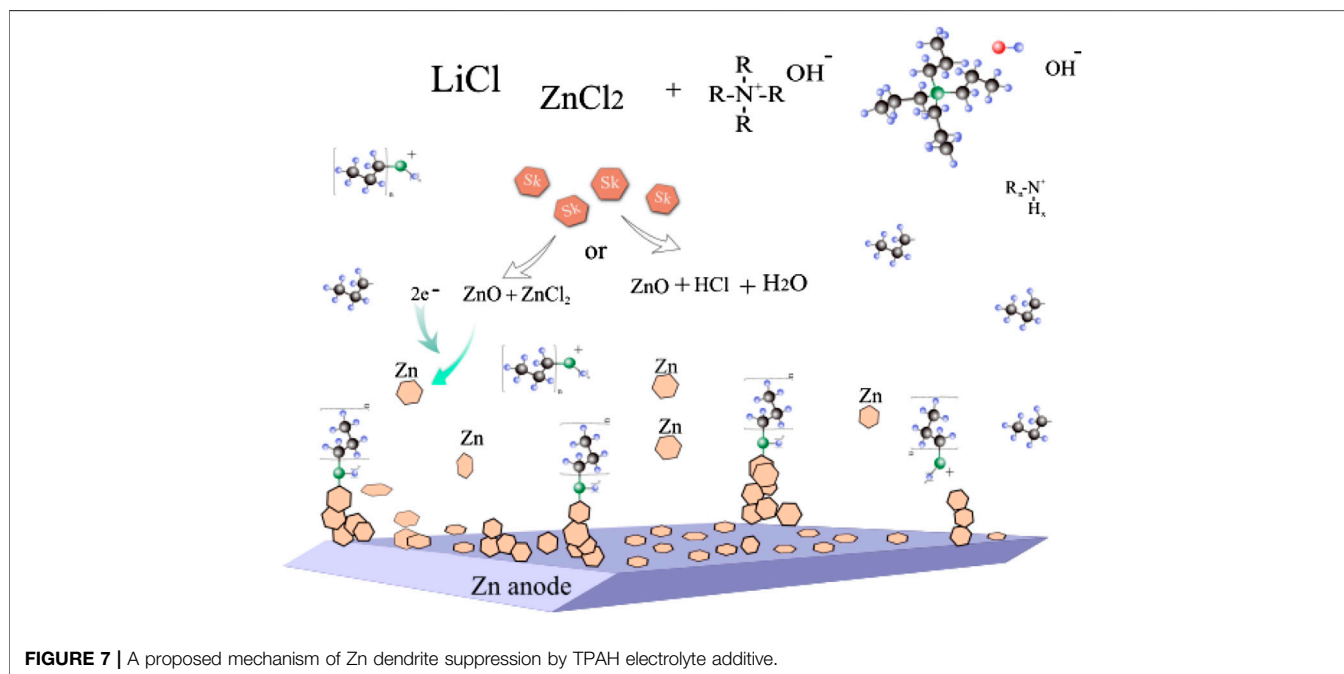
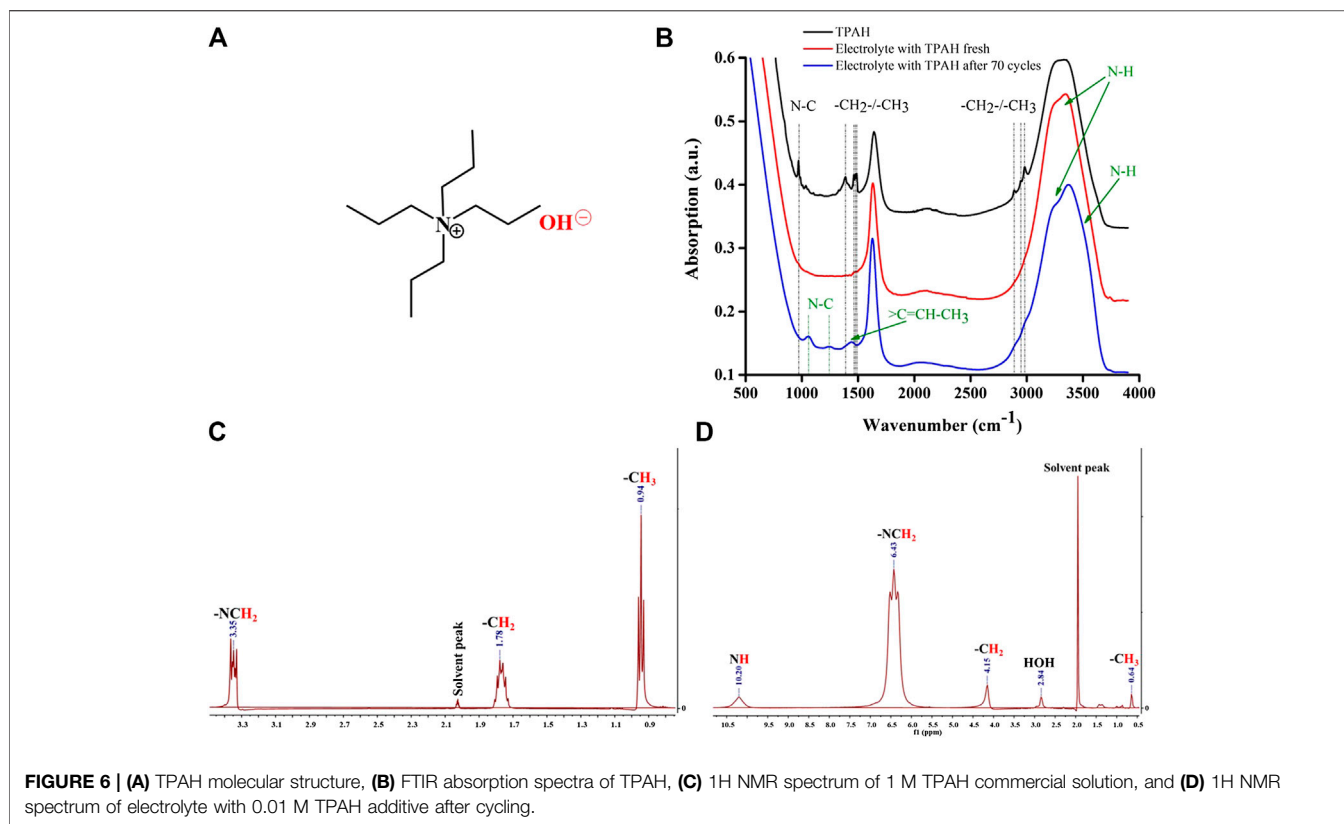
looser (**Figure 5D**). The high magnification images of Zn dendrites of both cells consist of the hexagonal disks (**Figures 5E,F**). The size of the disk is smaller in the left picture (about 1 μm in width), and they packed randomly and very close to each other like a sponge (**Figure 5C**). In the case of TPAH addition (**Figure 5F**), even distributed Zn disks have a size of 2–3 μm in width and they are much thicker than in **Figure 5C**.

Therefore, TPAH addition in electrolyte changed the distribution and structure of dendrites. With TPAH Zn dendrites grow on the surface of anode more uniformly. Dendrite aggregates on the surface of Zn anode of beaker cell with TPAH addition have almost the same size, even though they are cycled 70 times at 20°C. The beaker cell without TPAH short-circuited after 50 cycles due to the enlarged size of particular dendrites.

The electrolytes with TPAH before and after cycling were analyzed by FTIR and NMR. TPAH is a quaternary ammonium cation with four propyl substituents around the central nitrogen and hydroxyl group (**Figure 6A**). **Figure 6B** gives the FTIR spectra of the commercial TPAH, the electrolytes with TPAH before and after cycling. The peaks in the ranges of 1,630–1,650, 1,850–2,450, 3,200–3,500 cm^{-1} appear due to the water. The

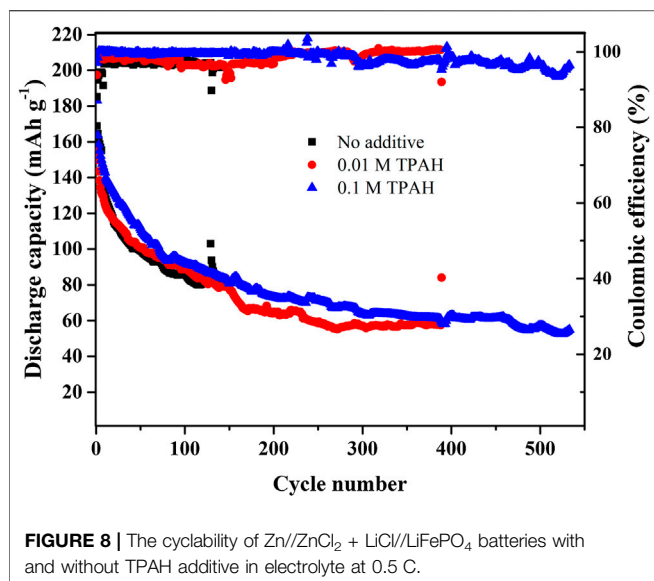
spectrum of commercial TPAH has its characteristic peaks due to propyl group (740–720, 1,390–1,375, 1,490–1,450, 3,000–2,850 cm^{-1}) and N-C vibrational mode (970–980 cm^{-1}) (**Figure 6B**, black line) (Spectroscopic Tools). When TPAH was added to ZnCl_2 and LiCl containing electrolyte, all corresponding to TPAH peaks disappear (**Figure 6B**, red line). We assume that aqueous electrolyte overloaded characteristic peaks, but new N-H vibration mode at 3,243 cm^{-1} (Zhai et al., 2006) is seen in solution of electrolyte before cycling. The ions in the solution interact with TPAH (**Supplementary Figure S4**) and break vibrational modes of N-C and propyl bonds. The cycled electrolyte shows several features. Shifted peaks appear at 1,050, 1,250 cm^{-1} , indicating the presence of amine groups in the electrolyte. In addition, the vibrational mode of $-\text{CH}=\text{CH}_2$ appears at 1,450 cm^{-1} , and the shoulder at 3,600 cm^{-1} which is ascribed to N-H vibration becoming more pronounced. These peaks confirm the aforementioned content of cycled electrolyte solution.

Figure 6 illustrates the ^1H NMR spectrum of (**C**) 1 M TPAH commercial solution and (**D**) electrolyte with 0.01 M TPAH after cycling, respectively. The ^1H NMR spectrum of initial TPAH is fully matched with published data (Tetrapropylammonium hydroxide - ^1H NMR Chemical Shifts - SpectraBase). The ^1H NMR spectrum of



electrolyte after cycling revealed signals corresponding to methyl proton at 0.64 (m), methylene proton at 4.15 (br s), methylene proton attached to N atom at 6.43 (t), and amine group proton at 10.21 (br s). The

structure of the propyl group attracted to N atom is assigned from the resonances at δH 0.64, 4.15, 6.43, and 10.21. From the NMR figures, we can observe the shifting of peaks that occurred due to the strong



resonance effect of the amine group. All the presented data suggested (predicted) that TPAH in electrolyte after cycling was decomposed to $R_n\text{-NH}$ and propene by comparison of spectra included in this study together with literature data (Spectroscopic Tools; Nishioka, 1974).

Based on all experimental results the following mechanism of the influence of TPAH addition to the electrolyte on battery cyclability is proposed (Figure 7). First, TPAH in electrolyte solution increased the yield of simonkolleite formation (Supplementary Figure S4). Simonkolleite is unstable and can decompose to ZnO and ZnCl₂ or to ZnO + HCl + H₂O (Zhang and Yanagisawa, 2007; Yoo et al., 2013; Moezzi et al., 2016). It is interesting to notice that simonkolleite disks appear with the combination of lower alkalinity, lower temperature, and higher NH_4^+ ions concentration and in existence of Cl^- anion (Li et al., 2011; Cousy et al., 2017). Second, when the battery starts to cycle at high C rate (20 C), Zn dendrites are formed on anode by applying a negative current. During the cycling TPAH decomposes to propylamine ($R_n\text{N}^+\text{H}$) and propene (Zhai et al., 2006; Prokopova et al., 2013). $R_n\text{N}^+\text{H}$ adsorbs on the active site of Zn dendrite, preventing its further growth (Lan et al., 2007). Zinc in battery with TPAH addition deposited mostly in a basal (parallel) oriented direction to anode surface.

The cyclability and the Coulombic efficiency of the batteries without additive and with the smallest and highest concentration of TPAH as 0.01 and 0.1 M at 0.5 C are shown in Figure 8. The Coulombic efficiency of all systems is high (96–100%).

The specific discharge capacity of all batteries gradually decreases with each cycle. However, the cell without the additive is inferior in terms of the stability. Batteries with TPAH (0.01 and 0.1 M) performed better cyclability, which are over 380 and 570 cycles, rather than the system with bare electrolyte. Apparently, the addition of the TPAH can prevent zinc dendrite growth, consequently prolonging cycle life of Zn/LiFePO₄ system.

CONCLUSION

In summary, the effect of TPAH as an electrolyte additive on the inhibition of Zn dendrite growth in aqueous rechargeable Li-ion battery Zn/LiFePO₄ has been investigated. The TPAH additive inhibits the dendritic growth on the Zn anode surface, increasing the battery life cycle. The mechanism of this process is proposed based on the results of SEM and XRD analysis of the Zn anode and FTIR and NMR studies of the electrolyte solution. The XRD pattern of the negative electrode of battery with TPAH indicates that Zn from electrolyte solution was preferentially deposited in a highly oriented (002) direction, which is more resistant to dendrite formation. Zn dendrites are deposited on the surface of anode more uniformly. During the electrochemical cycling TPAH decomposes to propylamine ($R_n\text{N}^+\text{H}$) and propene. They adsorb on the tip of Zn nucleation site and cover the surface of the electrode, preventing further growth of dendrite.

DATA AVAILABILITY STATEMENT

The original contributions presented in the study are included in the article/Supplementary Materials; further inquiries can be directed to the corresponding author/s.

AUTHOR CONTRIBUTIONS

AM and ZB contributed to conception and design of the study, IK analyzed data and contributed to the final version of the manuscript, KK carried out the experiment and wrote the first draft of the manuscript, and AA, LR, and DB carried out the experiment. All authors contributed to manuscript revision, read, and approved the submitted version.

FUNDING

This work was supported by the research grant AP05136016 “Zinc Based Rechargeable Aqueous Battery: A Green, Safe and Economic Battery for Space Applications (ZRABS)” and targeted the program BR05236524 “Innovative Materials and Systems for Energy Conversion and Storage” from the Ministry of Education and Science of the Republic of Kazakhstan.

ACKNOWLEDGMENTS

The authors thank their colleagues Dr. B. Uzakbaiuly and Dr. I. Trussov who greatly assisted the research with analytical techniques.

SUPPLEMENTARY MATERIAL

The Supplementary Material for this article can be found online at: <https://www.frontiersin.org/articles/10.3389/fenrg.2020.599009/full#supplementary-material>

REFERENCES

- Bani Hashemi, A., Kasiri, G., and La Mantia, F. (2017). The effect of polyethyleneimine as an electrolyte additive on zinc electrodeposition mechanism in aqueous zinc-ion batteries. *Electrochim. Acta.* 258, 703–708. doi:10.1016/j.electacta.2017.11.116
- Batyrbekuly, D., Cajoly, S., Läik, B., Pereira-Ramos, J., Emery, N., Bakenov, Z., et al. (2020). Mechanistic investigation of a hybrid Zn/V₂O₅ rechargeable battery with a binary Li⁺/Zn²⁺ aqueous electrolyte. *ChemSusChem.* 13, 724–731. doi:10.1002/cssc.201903072
- Beck, F., and Rüetschi, P. (2000). Rechargeable batteries with aqueous electrolytes. *Electrochim. Acta.* 45, 2467–2482. doi:10.1016/S0013-4686(00)00344-3
- Cousy, S., Gorodylova, N., Svoboda, L., and Zelenka, J. (2017). Influence of synthesis conditions over simonkolleite/ZnO precipitation. *Chem. Pap.* 71, 2325–2334. doi:10.1007/s11696-017-0226-4
- Fang, G., Zhou, J., Pan, A., and Liang, S. (2018). Recent advances in aqueous zinc-ion batteries. *ACS Energy Lett.* 3, 2480–2501. doi:10.1021/acsenerylett.8b01426
- Garcia, G., Ventosa, E., and Schuhmann, W. (2017). Complete prevention of dendrite formation in Zn metal anodes by means of pulsed charging protocols. *ACS Appl. Mater. Interfaces.* 9, 18691–18698. doi:10.1021/acsami.7b01705
- Gomes, A., and da Silva Pereira, M. I. (2006). Zn electrodeposition in the presence of surfactants. Part I. Voltammetric and structural studies. *Electrochim. Acta.* 52, 863–871. doi:10.1016/j.electacta.2006.06.025
- Higashi, S., Lee, S. W., Lee, J. S., Takechi, K., and Cui, Y. (2016). Avoiding short circuits from zinc metal dendrites in anode by backside-plating configuration. *Nat. Commun.* 7, 1–6. doi:10.1038/ncomms11801
- Hoang, T. K. A., Acton, M., Chen, H. T. H., Huang, Y., Doan, T. N. L., and Chen, P. (2017). Sustainable gel electrolyte containing Pb²⁺ as corrosion inhibitor and dendrite suppressor for the zinc anode in the rechargeable hybrid aqueous battery. *Mater. Today Energy.* 4, 34–40. doi:10.1016/j.mtener.2017.03.003
- Hu, P., Yan, M., Zhu, T., Wang, X., Wei, X., Li, J., et al. (2017). Zn/V₂O₅ aqueous hybrid-ion battery with high voltage platform and long cycle life. *ACS Appl. Mater. Interfaces.* 9, 42717–42722. doi:10.1021/acsami.7b13110
- Kan, J., Xue, H., and Mu, S. (1998). Effect of inhibitors on Zn-dendrite formation for zinc-polyaniline secondary battery. *J. Power Sources.* 74, 113–116. doi:10.1016/S0378-7753(98)00040-8
- Konarov, A., Voronina, N., Jo, J. H., Bakenov, Z., Sun, Y. K., and Myung, S. T. (2018). Present and future perspective on electrode materials for rechargeable zinc-ion batteries. *ACS Energy Lett.* 3, 2620–2640. doi:10.1021/acsenerylett.8b01552
- Lan, C. J., Lee, C. Y., and Chin, T. S. (2007). Tetra-alkyl ammonium hydroxides as inhibitors of Zn dendrite in Zn-based secondary batteries. *Electrochim. Acta.* 52, 5407–5416. doi:10.1016/j.electacta.2007.02.063
- Li, H., Ma, L., Han, C., Wang, Z., Liu, Z., Tang, Z., et al. (2019a). Advanced rechargeable zinc-based batteries: recent progress and future perspectives. *Nanomater. Energy.* 62, 550–587. doi:10.1016/j.nanoen.2019.05.059
- Li, M., He, Q., Li, Z., Li, Q., Zhang, Y., Meng, J., et al. (2019b). A novel dendrite-free Mn²⁺/Zn²⁺ hybrid battery with 2.3 V voltage window and 11000-cycle lifespan. *Adv. Energy Mater.* 9, 1–10. doi:10.1002/aenm.201901469
- Li, S., Chen, X., Wang, X., Xiong, Y., Yan, Y., Tan, Z., et al. (2019c). Simonkolleite coating on poly(amino acids) to improve osteogenesis and suppress osteoclast formation *in vitro*. *Polymers (Basel).* 11, 1505. doi:10.3390/polym11091505
- Li, Y., Zou, Y., and Hou, Y. (2011). Synthesis and characterization of simonkolleite nanodisks and their conversion into ZnO nanostructures. *Cryst. Res. Technol.* 46, 305–308. doi:10.1002/crat.201000673
- Lu, W., Xie, C., Zhang, H., and Li, X. (2018). Inhibition of zinc dendrite growth in zinc-based batteries. *ChemSusChem.* 11, 3996–4006. doi:10.1002/cssc.201801657
- Mitha, A., Mi, H., Dong, W., Cho, I. S., Ly, J., Yoo, S., et al. (2019). Thixotropic gel electrolyte containing poly(ethylene glycol) with high zinc ion concentration for the secondary aqueous Zn/LiMn₂O₄ battery. *J. Electroanal. Chem.* 836, 1–6. doi:10.1016/j.jelechem.2019.01.014
- Mitha, A., Yazdi, A. Z., Ahmed, M., and Chen, P. (2018). Surface adsorption of polyethylene glycol to suppress dendrite formation on zinc anodes in rechargeable aqueous batteries. *ChemElectroChem.* 5, 2409–2418. doi:10.1002/celec.201800572
- Moezzi, A., Cortie, M., and McDonagh, A. (2016). Transformation of zinc hydroxide chloride monohydrate to crystalline zinc oxide. *Dalton Trans.* 45, 7385–7390. doi:10.1039/c5dt04864h
- Moser, F., Fourgeot, F., Rouget, R., Crosnier, O., and Brousse, T. (2013). *In situ* X-ray diffraction investigation of zinc based electrode in Ni-Zn secondary batteries. *Electrochim. Acta.* 109, 110–116. doi:10.1016/j.electacta.2013.07.023
- Nayana, K. O., and Venkatesha, T. V. (2011). Synergistic effects of additives on morphology, texture and discharge mechanism of zinc during electrodeposition. *J. Electroanal. Chem.* 663, 98–107. doi:10.1016/j.jelechem.2011.10.001
- Nayana, K. O., and Venkatesha, T. V. (2015). Bright zinc electrodeposition and study of influence of synergistic interaction of additives on coating properties. *J. Ind. Eng. Chem.* 26, 107–115. doi:10.1016/j.jiec.2014.11.021
- Nishioka, A. (1974). High resolution NMR. San Diego, CA: Academic Press. doi:10.1295/kobunshi.23.310
- Parker, J. F., Chervin, C. N., Pala, I. R., Machler, M., Burz, M. F., Long, J. W., et al. (2017). Rechargeable nickel–3D zinc batteries: an energy-dense, safer alternative to lithium-ion. *Science.* 356, 415–418. doi:10.1126/science.aak9991
- Prokopova, O., Bernauer, B., Frycova, M., Hrabanek, P., Zikanova, A., and Kocirik, M. (2013). Principal features of tetrapropylammonium hydroxide removal kinetics from silicalite-1 in quasi-isothermal heating regimes. *J. Phys. Chem. C.* 117, 1468–1476. doi:10.1021/jp3090364
- Science and Fun. Spectroscopic tools. Available at: <https://www.science-and-fun.de/tools/> (Accessed July 20, 2020).
- Shin, J., Lee, J., Park, Y., and Choi, J. W. (2020). Aqueous zinc ion batteries: focus on zinc metal anodes. *Chem. Sci.* 11, 2028–2044. doi:10.1039/d0sc00022a
- SpectraBase. Tetrapropylammonium hydroxide-1H NMR chemical shifts. Available at: <https://spectrabase.com/spectrum/KLXRcA3Yuni> (Accessed July 20, 2020).
- Sun, K. E. K., Hoang, T. K. A., Doan, T. N. L., Yu, Y., and Chen, P. (2018). Highly sustainable zinc anodes for a rechargeable hybrid aqueous battery. *Chem. A Eur. J.* 24, 1667–1673. doi:10.1002/chem.201704440
- Wang, F., Borodin, O., Gao, T., Fan, X., Sun, W., Han, F., et al. (2018a). Highly reversible zinc metal anode for aqueous batteries. *Nat. Mater.* 17, 543–549. doi:10.1038/s41563-018-0063-z
- Wang, K., Pei, P., Wang, Y., Liao, C., Wang, W., and Huang, S. (2018b). Advanced rechargeable zinc-air battery with parameter optimization. *Appl. Energy.* 225, 848–856. doi:10.1016/j.apenergy.2018.05.071
- Wang, Y., Niu, Z., Zheng, Q., Zhang, C., Ye, J., Dai, G., et al. (2018c). Zn-based eutectic mixture as anolyte for hybrid redox flow batteries. *Sci. Rep.* 8, 8–15. doi:10.1038/s41598-018-24059-x
- Wang, M., Emre, A., Tung, S., Gerber, A., Wang, D., Huang, Y., et al. (2019). Biomimetic solid-state Zn²⁺ electrolyte for corrugated structural batteries. *ACS Nano.* 13, 1107–1115. doi:10.1021/acsnano.8b05068
- Xu, C., Li, B., Du, H., and Kang, F. (2012). Energetic zinc ion chemistry: the rechargeable zinc ion battery. *Angew. Chem. Int. Ed.* 51, 933–935. doi:10.1002/anie.201106307
- Xu, M., Ivey, D. G., Qu, W., and Xie, Z. (2015). Study of the mechanism for electrodeposition of dendrite-free zinc in an alkaline electrolyte modified with 1-ethyl-3-methylimidazolium dicyanamide. *J. Power Sources.* 274, 1249–1253. doi:10.1016/j.jpowsour.2014.10.140
- Yan, J., Wang, J., Liu, H., Bakenov, Z., Gosselink, D., and Chen, P. (2012). Rechargeable hybrid aqueous batteries. *J. Power Sources.* 216, 222–226. doi:10.1016/j.jpowsour.2012.05.063
- Yesibolati, N., Umirov, N., Koishybay, A., Omarova, M., Kurmanbayeva, I., Zhang, Y., et al. (2015). High performance Zn/LiFePO₄ aqueous rechargeable battery for large scale Applications. *Electrochim. Acta.* 152, 505–511. doi:10.1016/j.electacta.2014.11.168
- Yoo, J. D., Volovitch, P., Abdel Aal, A., Allely, C., and Ogle, K. (2013). The effect of an artificially synthesized simonkolleite layer on the corrosion of electrogalvanized steel. *Corrosion Sci.* 70, 1–10. doi:10.1016/j.corsci.2012.10.024
- Yufit, V., Tariq, F., Eastwood, D. S., Biton, M., Wu, B., Lee, P. D., et al. (2019). Operando visualization and multi-scale tomography studies of dendrite formation and dissolution in zinc batteries. *Joule.* 3, 485–502. doi:10.1016/j.joule.2018.11.002

- Zeng, X., Hao, J., Wang, Z., Mao, J., and Guo, Z. (2019). Recent progress and perspectives on aqueous Zn-based rechargeable batteries with mild aqueous electrolytes. *Energy Storage Mater.* 20, 410–437. doi:10.1016/j.ensm.2019.04.022
- Zhai, J. P., Tang, Z. K., Li, Z. M., Li, I. L., Jiang, F. Y., Sheng, P., et al. (2006). Carbonization mechanism of tetrapropylammonium-hydroxide in channels of $\text{AlPO}_4\cdot 5$ single crystals. *Chem. Mater.* 18, 1505–1511. doi:10.1021/cm0526821
- Zhang, N., Chen, X., Yu, M., Niu, Z., Cheng, F., and Chen, J. (2020). Materials chemistry for rechargeable zinc-ion batteries. *Chem. Soc. Rev.* 49, 4203–4219. doi:10.1039/c9cs00349e
- Zhang, N., Cheng, F., Liu, J., Wang, L., Long, X., Liu, X., et al. (2017). Rechargeable aqueous zinc-manganese dioxide batteries with high energy and power densities. *Nat. Commun.* 8, 405. doi:10.1038/s41467-017-00467-x
- Zhang, W., and Yanagisawa, K. (2007). Hydrothermal synthesis of zinc hydroxide chloride sheets and their conversion to ZnO. *Chem. Mater.* 19, 2329–2334. doi:10.1021/cm0626841
- Zhou, Z., Zhang, Y., Chen, P., Wu, Y., Yang, H., Ding, H., et al. (2019). Graphene oxide-modified zinc anode for rechargeable aqueous batteries. *Chem. Eng. Sci.* 194, 142–147. doi:10.1016/j.ces.2018.06.048
- Zhu, H. W., Ge, J., Peng, Y. C., Zhao, H. Y., Shi, L. A., and Yu, S. H. (2018). Dip-coating processed sponge-based electrodes for stretchable Zn-MnO₂ batteries. *Nano Res.* 11, 1554–1562. doi:10.1007/s12274-017-1771-4

Conflict of Interest: Authors IK, KK, AM and ZB were employed by company Institute of Batteries LLP.

The remaining authors declare that the research was conducted in the absence of any commercial or financial relationships that could be construed as a potential conflict of interest.

Copyright © 2020 Kurmanbayeva, Rakhymbay, Korzhynbayeva, Adi, Batyrbekuly, Mentbayeva and Bakenov. This is an open-access article distributed under the terms of the Creative Commons Attribution License (CC BY). The use, distribution or reproduction in other forums is permitted, provided the original author(s) and the copyright owner(s) are credited and that the original publication in this journal is cited, in accordance with accepted academic practice. No use, distribution or reproduction is permitted which does not comply with these terms.